ACS APPLIED MATERIALS & INTERFACES

Research Article

www.acsami.org

Pulsed-Laser Desorption/Ionization of Clusters from Biofunctional Gold Nanoparticles: Implications for Protein Detections

Yin-Chun Liu,[†] Huan-Tsung Chang,[‡] Cheng-Kang Chiang,[‡] and Chih-Ching Huang*[,†,§]

[†]Institute of Bioscience and Biotechnology and [§]Center of Excellence for Marine Bioenvironment and Biotechnology (CMBB), National Taiwan Ocean University, Keelung, Taiwan

[‡]Department of Chemistry, National Taiwan University, Taipei, Taiwan

Supporting Information

ABSTRACT: In this paper, we describe a pulsed-laser desorption/ionization mass spectrometry (LDI-MS) approach for the detection of proteins with femtomolar sensitivity through the analysis of gold (Au) clusters desorbed from aptamer-modified gold nanoparticles (Apt–AuNPs) on a nitrocellulose membrane (NCM). After the target protein (thrombin) was selectively captured by the surface-bound 29-mer thrombin-binding aptamer (TBA_{29}), the thrombin/TBA_{29}–AuNP complexes were concentrated and deposited onto the NCM to form a highly efficient background-free surface-assisted LDI substrate. Under pulsed laser irradiation (355 nm), the binding of thrombin decreased the desorption and/or ionization efficiencies of the Au atoms from the AuNP surfaces. The resulting decreases in the intensities of the signals for Au clusters in the mass spectra provided a highly amplified target-labeling indicator for the targeted protein. Under optimized conditions, this probe was highly sensitive (limit of detection: ca. 50 fM) and selective (by at least 1000-fold over other proteins) toward thrombin; it also improved reproducibility (<5%) of ion production by presenting a more-homogeneous substrate surface, thereby enabling LDI-based measurements for the accurate and precise quantification of thrombin in human serum. This novel LDI-MS approach allows high-speed analyses of low-abundance thrombin with ultrahigh sensitivity; decorating the AuNP surfaces with other aptamers also allowed amplification of other biological signals.

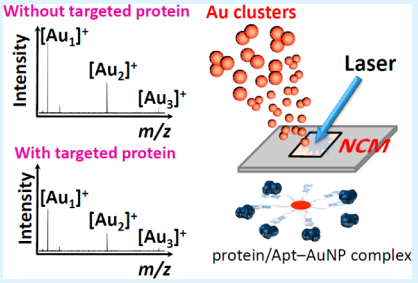

KEYWORDS: *pulsed-laser desorption, gold nanoparticles, clusters, aptamers, proteins*

INTRODUCTION

Relative to bulk gold (Au) materials, gold nanoparticles (AuNPs), with typical sizes of 1–100 nm, display unique physical and chemical properties, mainly because of unusual quantum effects.[1,2] To date, AuNPs have been the most commonly used optical sensing nanomaterials because of their strong surface plasmon resonance (SPR) absorption in the visible region, ease of sample preparation, and high stability and biocompatibility.[3−6] In addition, the surface chemistry of AuNPs is versatile, allowing the linking of various biofunctional groups (e.g., sugars, peptides, lipids, proteins, nucleic acids) through Au–S or Au–N bonding or physical adsorption.[3−6]

Another application of AuNPs is in the field of mass spectrometry (MS)—in particular, surface-assisted laser desorption/ionization mass spectrometry (SALDI-MS),[7,8] a well-known organic matrix–free approach that uses nanoparticles (NPs) or substrate materials to mediate desorption processes. SALDI-MS is a promising means of analyzing compounds in the low mass range (m/z < 500).[7−15] Several nanomaterials with various sizes, shapes, and compositions have been adopted as SALDI matrices because of their suitability for analytical and bioanalytical applications.[16−20] Surface-assisted laser desorption/ionization mass spectrometry (SALDI-MS) using AuNPs as matrices have been widely employed for the analyses of various molecules of interest (e.g., aminothiols, carbohydrates, peptides, proteins) by monitoring the analytes signals in MS spectra.[8,25−33] Despite the attractions and the promising results achieved with Au NP–assisted laser desorption/ionization (LDI), thermally driven energy transfer from the Au NP substrates to the analytes is generally accompanied by the production of many Au cluster ions ($[Au_x]^+$; x = 1–25).[25−33] As a result, the signals of the sample ions were suppressed dramatically, forming complicated mass spectra, and, thereby, lowering the analytical sensitivity. In addition, the mass limit remains rather low (<25 kDa) in AuNP-based LDI-MS approaches.[8,34] In this present study, in order to provide additional chemical information regarding the surface structures of Au NPs, we employed SALDI-MS with Au NPs as matrices to study the interactions between proteins and aptamer-modified Au NPs (Apt–Au NPs). We used the signal intensity of the Au clusters from Apt–AuNPs as a target-labeling indicator for proteins.

Thrombin is a key enzyme in the coagulation cascade, which converts soluble fibrinogen into insoluble strands of fibrin and catalyzes many other coagulation-related reactions, including direct activation of protein C and platelets and feedback

Received: June 30, 2012
Accepted: September 21, 2012
Published: September 21, 2012

   dx.doi.org/10.1021/am3011934 | ACS Appl. Mater. Interfaces 2012, 4, 5241–5248

activation of procofactors V and VIII.[35] Thrombin is also involved in anticoagulation and fibrinolysis, tissue repair and wound healing, progression of neoplasia, inflammation, tumor implantation, tumor cell growth, and metastasis.[36] Thrombin is a useful tumor marker for the diagnosis of tumor growth, metastasis, and angiogenesis,[37] but its detection is difficult, mainly because its concentration in blood can vary considerably; indeed, it is not present in blood under normal conditions.[38−40] During a coagulation reaction, the concentration of free thrombin can range from less than 1 nM to greater than 500 nM.[38] Apart from the hemostatic process, thrombin circulates at the high-picomolar level in the blood of patients suffering from diseases known to be associated with coagulation abnormalities.[38−40] Thus, we are interested in approaches for the rapid detection of thrombin in blood at picomolar concentrations over a wide dynamic range.

In this study, we developed an energy transduction strategy that combines Apt−AuNPs with LDI-MS, without additional amplification or target-labeling steps, for the detection of a target protein (thrombin) in a solution. In our approach, thrombin was captured selectively by aptamers present on AuNP surfaces;[41] the particles were subsequently deposited onto a nitrocellulose membrane (NCM) to form a highly efficient background-free SALDI substrate (Scheme 1). Under

Scheme 1. Schematic Representation of the Preparation of the TBA_{29}−AuNP/NCM Substrate and Its Use, In Conjunction with LDI-MS, for the Analysis of Thrombin[a]

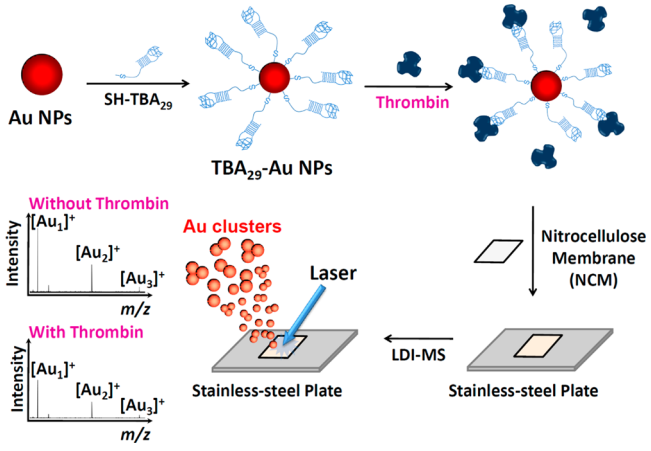

[a]TBA_{29} is the 29-base thrombin-binding aptamer.

pulsed-laser irradiation (Nd:YAG, 355 nm), the efficiency of Au cluster formation was diminished in the presence of the target proteins. Accordingly, we used the decrease in the signal intensity of the Au clusters as a target-labeling indicator for thrombin. These Au-cluster-driven signals were considerably stronger than those of the target protein itself—often difficult to analyze using MS because of the protein's low ionization/desorption efficiency, even when present in high concentrations. The use of the homogeneous Apt−AuNP/NCM nanocomposite can provide high reproducibility and clean mass spectra of Au cluster ions with fewer and weaker signals from interfering species.[42] Under optimized conditions, we used our new method as an analytical tool for the sensitive and selective detection of thrombin in a representative serum sample.

EXPERIMENTAL SECTION

Chemicals. Calcium chloride ($CaCl_2$), magnesium chloride ($MgCl_2$), potassium chloride (KCl), sodium chloride (NaCl), tris(hydroxymethyl)aminomethane (Tris), trisodium citrate, and hydrochloric acid (HCl) were purchased from Mallinckrodt Baker (Phillipsburg, NJ, USA). Sodium tetrachloroaurate(III) ($NaAuCl_4$) was purchased from Aldrich (Milwaukee, WI). The oligonucleotide-labeling dye OliGreen (OG) was obtained from Molecular Probes (Portland, OR). Human α-thrombin (≥1000 NIH units/mg protein), lysozyme, and bovine serum albumin (BSA) were obtained from Sigma (St. Louis, MO, USA). Nucleolin was purchased from Abcam (Cambridge, MA, USA). Recombinant platelet-derived growth factor BB (PDGF-BB) was purchased from R&D Systems (Minneapolis, MN, USA). All oligonucleotides and thiol-modified oligonucleotides listed in Table 1 were purchased from Integrated DNA Technologies

Table 1. DNA Sequences of TBA_{29}, Apt_{PDGF}, AGRO100, and Apt_{Lys} Used in This Study

name	sequence
TBA_{29}	5′-SH-TTT TTT TTT TTT TTT ATC TAG TCC GTG GTA GGG CAG GTT GGG GTG ACT AGA T-3′
Apt_{PDGF}	5′-SH-TTT TTT TTT TTT TTT CAG GCT ACG GCA CGT AGA GCA TCA CCA TGA TCC TG-3′
AGRO100	5′-SH-TTT TTT TTT TTT TTT GGT GGT GGT GGT TGT GGT GGT GGT GG-3′
Apt_{Lys}	5′-SH-TTT TTT TTT TTT TTT ATC TAC GAA TTC ATC AGG GCT AAA GAG TGC AGA GTT ACT TAG-3′

(Coralville, IA, USA). Amersham Hybond-C Extra NCM (pore size: 0.45 μM) was purchased from GE Healthcare Bioscience (Buckinghamshire, UK). All other reagents used in this study were purchased from Aldrich (Milwaukee, WI, USA). All solvents and chemicals were of the highest purity available commercially and used without further purification. Milli-Q ultrapure water was used in each experiment.

Preparation and Characterization of AuNPs. Spherical AuNPs (diameter: 13.3 nm) were prepared through 4.0 mM citrate-mediated reduction of 1.0 mM $NaAuCl_4$. Their sizes were verified using an H7100 transmission electron microscope (Hitachi High-Technologies, Tokyo, Japan); the AuNPs appeared to be nearly monodisperse with an average diameter of 13.3 (±1.2) nm. A Cintra 10e double-beam UV−Vis spectrophotometer (GBC, Victoria, Australia) was used to measure the absorptions of AuNP solutions. The AuNP particle concentration (15 nM) was determined using Beer's law with an extinction coefficient of 2.08×10^8 M^{-1} cm^{-1} at 520 nm for the 13.3 nm AuNPs. Preparation of 32- and 56-nm AuNPs: 1% trisodium citrate solutions (0.5 and 0.3 mL, respectively) were added rapidly to 0.01% $NaAuCl_4$ solutions (50 mL) under reflux in flasks equipped with reflux condensers. The solutions were heated under reflux for another 8 min, during which time they changed color to pink (32 nm) and purple (56 nm), respectively. The particle concentrations of the 32- and 56-nm Au NPs were 280 and 54 pM, respectively. Dynamic light scattering (DLS) data and zeta potentials of the Au NPs were measured using a Zetasizer 3000HS analyzer (Malvern Instruments, Malvern, UK).

Preparation of TBA_{29}−AuNPs. Thiol-modified DNA samples—including 29-base thrombin-binding aptamers (TBA_{29}) that bind to exosite 2 of thrombin, PDGF-BB−binding aptamers (Apt_{PDGF}), nucleolin-binding aptamers (AGRO100), and lysozyme-binding aptamers (Apt_{Lys})—were attached separately to AuNPs using a modified procedure.[43] The 5′-thiol−modified oligonucleotides received in the disulfide form [$HOCH_3(CH_2)_5S$−S−3′-oligo] were reacted directly with the AuNPs, attaching both their $HO(CH_2)_6S$ and oligo-S units onto each AuNP surface. For example, aliquots of aqueous AuNP solutions (15 nM, 1000 μL) in 1.5-mL tubes were mixed with SH(thiol)-TBA_{29} (100 μM, 20 μL). After 2 h at room temperature, 200 mM NaCl was added to the solutions, which were incubated for 10 h (salt aging) to form TBA_{29}−AuNPs. Salt aging

resulted in higher numbers of aptamer molecules bound to each AuNP.[44] The mixtures were centrifuged (relative centrifugal force: 30 000 *g*; 20 min) to remove unattached thiol oligonucleotides. The supernatants were removed and the oily precipitates washed with Tris-HCl (pH 7.4, 5.0 mM, 1.0 mL). After three centrifuge/wash cycles, the colloids (TBA_{29}–AuNPs) were resuspended separately in Tris-HCl (pH 7.4, 5.0 mM, 1.0 mL). The purified TBA_{29}–AuNP was stable for at least 3 months when stored at 4 °C in the dark. DLS measurements (n = 5) suggested that the hydrodynamic diameters of the unlabeled AuNPs and TBA_{29}–AuNP assemblies were 17.7 (±4.7) and 44.3 (±2.1) nm, respectively. To determine the number of oligonucleotide molecules attached to each AuNP, 2-mercaptoethanol (10 mM) was added to displace the oligonucleotides from the surfaces of the AuNPs through an exchange reaction. The solution containing the displaced oligonucleotides was then separated from the AuNPs through centrifugation (30 000 *g*, 20 min). The concentration of oligonucleotide molecules displaced from the TBA_{29}–AuNPs was determined through the addition of OliGreen (OG),[45] which exhibits a greater-than-1000-fold enhancement in its fluorescence at 524 nm upon binding to oligonucleotides when excited at 480 nm. This analysis suggested that 70 oligonucleotide molecules were attached to each AuNP.

Detection of Thrombin through LDI-MS with TBA_{29}–AuNP/NCM as Substrate. Thrombin (0–10 nM) was preincubated at room temperature with 10 pM TBA_{29}–AuNPs (10 pM AuNPs; ca. 700 pM TBA_{29}) in biological buffer [25 mM Tris-HCl (pH 7.4), 150 mM NaCl, 5.0 mM KCl, 1.0 mM $MgCl_2$, 1.0 mM $CaCl_2$; 0.5 mL] in the presence of BSA (100 μM) for 2 h. A piece of NCM was cut to a size of 0.5 cm (length) × 0.5 cm (width) and then immersed in the solution (0.5 mL) in a 1.5 mL tube. After incubation for 2 h, the TBA_{29}–AuNP-adsorbed NCM (TBA_{29}–AuNP/NCM) was gently washed with deionized (DI) water (ca. 5 mL) for 30 s and dried for 1 min using an air gun (60 lb in.$^{-2}$). Au ions were not detected when analyzing the washing solution using inductively coupled plasma mass spectrometry (ICP-MS), indicating that the TBA_{29}–AuNPs were not released from the NCM during the washing steps. The NCM substrate was then attached to a matrix-assisted LDI (MALDI) plate using an adhesive polyimide film tape.

MS experiments were performed in the reflectron positive-ion or negative-ion mode using an AutoflexIII MALDI time-of-flight (TOF)/TOF mass spectrometer (Bruker Daltonics, Bremen, Germany). The samples were irradiated with a SmartBeam laser (Nd:YAG, 355 nm, pulse width 6 ns, pulse duration 200 ns) at 100 Hz. Ions produced by laser desorption were stabilized energetically during a delayed extraction period of 30 ns and then accelerated through the TOF chamber in the reflection mode prior to entering the mass analyzer. The available accelerating voltages ranged from +20 to −20 kV. The instruments were calibrated with Au clusters using their theoretical mass values ($[Au_x]^+$; x = 1–3). A total of 1000 pulsed laser shots were applied to accumulate signals from 10 MALDI target positions under a laser power density of 3.8×10^4 W cm^{-2}.

Analysis of Serum Samples. Serum samples from a healthy volunteer (26-year-old male) were drawn from a vein into a BD Vacutainer SST tube; within 0.5 h of collection they were centrifuged (3000 *g*, 10 min) at 4 °C. 10-fold-diluted serum samples (500 μL; without any treatment) were equilibrated and then spiked with standard thrombin solutions containing TBA_{29}–AuNPs (10 pM) in a biological buffer in the presence of BSA (100 μM) for 1 h. The final thrombin concentrations ranged from 1.0 fM to 10 nM. Subsequently, the samples were centrifuged and the supernatants removed. Each precipitate was resuspended in biological buffer (pH 7.4, 500 μL) and then the NCM was immersed in the solution in a 1.5 mL tube. After incubation for 2 h, the TBA_{29}–AuNP/NCM was gently washed with DI water (ca. 5 mL) for 30 s and dried for 1 min using an air gun (60 lb in.$^{-2}$). This substrate was attached to a MALDI plate using an adhesive polyimide film tape prior to LDI-MS measurement.

RESULTS AND DISSCUSION

Binding Thrombin to TBA_{29}–AuNPs. TBA-modified AuNPs (TBA–AuNPs) have been prepared previously and employed to detect and control the activity of thrombin.[46−50] Two well-known TBAs possess 15 (TBA_{15}) and 29 (TBA_{29}) bases that bind to exosite 1 and exosite 2 with dissociation constants (K_d) of approximately 100 and 0.5 nM, respectively.[41] We have found that TBA_{29}–P_8T_{15}–AuNPs (AuNPs conjugated with TBA_{15} and TBA_{29}; 15 thymine (T) units in the linker and eight stem pairs (P) at the termini of the TBAs) interact strongly with thrombin, with both reproducibility and repeatability.[50] For simplicity, here we use the descriptor "TBA_{29}–AuNPs" to represent AuNPs conjugated with approximately 70 TBA_{29} units presenting T_{15} and P_8. We chose TBA_{29}–AuNPs as affinity probes that would inhibit AuNP aggregation, with ultrahigh binding affinity toward thrombin (K_d < 0.01 nM), because of the high local concentration of TBA ligands on the particles' surfaces and the strong electrostatic interactions between TBA_{29}–AuNPs and thrombin.[46,47,50] In our previous studies,[46,47] we have found TBA density on Au NP had a strong influence on the binding affinity toward thrombin. Having higher TBA ligand densities on their surfaces resulted in stronger binding affinity because of a higher local concentration of TBA ligands on the particle's surface. When the surface density was low (<40), TBA ligands existed in the flattened structures, leading to weak affinity toward thrombin. On the other hand, when TBA–Au NPs presented more than 100 TBA molecules per Au NP, stretched, linear TBA structures predominated Au NP surfaces, and thus lowering their binding affinity.

Sensing Thrombin through LDI-MS with TBA_{29}–AuNPs as Substrates. Scheme 1 outlines the preparation of the TBA_{29}–AuNP/NCM substrate for the detection of thrombin using LDI-MS. NCMs are widely used as blotting matrices for protein immobilization,[51] with hydrophobic interactions being mainly responsible for the adsorption of proteins onto the NCM, allowing impurities to be removed through washing. After the TBA_{29}–AuNPs (10 pM) had interacted with thrombin in the presence of BSA (100 μM), we immersed the NCM (0.5 × 0.5 cm^2) in the TBA_{29}–AuNP solution for 2 h. In a previous study, we found that excess BSA in the solution stabilized the AuNPs through electrostatic attraction, providing superior salt- and protein-tolerance and improved homogeneity when they were adsorbed onto NCM surfaces.[42] The isoelectric point (pI) of BSA is 4.6 and therefore the BSA has negative net charge in biological buffer (pH 7.4). Regardless of the overall charge, BSA has 60 surface lysine groups that can have electrostatic interactions with negatively charged moieties. Thus, the adsorption of BSA to Au NPs is established through electrostatic interaction between the anionic groups on the nanoparticles and the positively charged amino groups of lysine residues of BSA. Apart from the electrostatic interaction, ionic/hydrogen bonding between $-NH_3^+$ and $-COO^-$-capped surface is also possible.

After the selective capture of thrombin by the TBA units on the AuNPs, the as-prepared TBA_{29}–AuNP/NCM substrate was subsequently analyzed using LDI-MS. The TBA_{29}–AuNPs served as SALDI matrices and produced Au cluster peaks ($[Au_x]^+$) in the mass spectrum, because Au clusters also desorbed from the target plate when the AuNPs were irradiated with a pulsed laser. In the presence of thrombin, however, the AuNPs transferred their energy to the surface thrombin

molecules, evaporation of surface atoms into the gas phase were suppressed, thereby resulting in low abundances for the signals of Au clusters in the mass spectrum. We also performed MS experiments under the reflectron negative-ion mode. However, no characteristic peaks of Au anion cluster peaks ($[Au_x]^-$) was detected in negative-ion mode (data not shown). This phenomenon occurs mainly because relative low ionization efficiency of negative Au cluster under pulsed laser irradiation when compared to those of positive Au cluster ions.[52−54] Accordingly, we could use the decreases in signal intensities of the positive Au clusters as an indicator of the target protein. Because the number of surface Au atoms (ca. 6,600) was greater than the number of proteins (ca. 50) on each 13 nm AuNP, the changes in the intensities of the Au clusters was greater than those of the analytes, thereby allowing this MS method to provide highly amplified signals for the sensitive (femtomolar range) and selective detection of thrombin.

Figure 1 compares the positive-ion mass spectra of TBA_{29}−AuNPs (10 pM) obtained using a stainless-steel MALDI plate

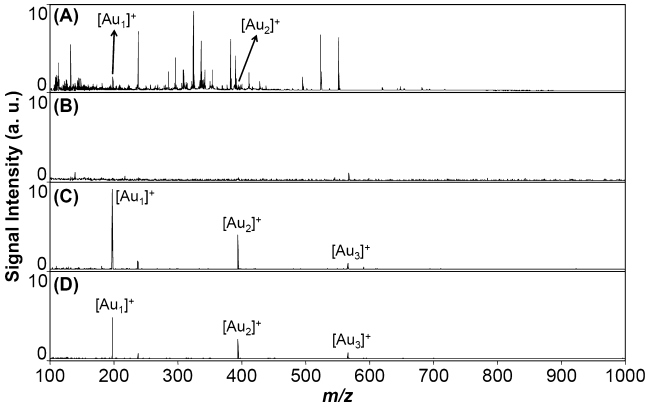

Figure 1. Mass spectra of (A) TBA_{29}−AuNPs (10 pM), (B) NCM, and (C, D) TBA_{29}−AuNP/NCM in the (C) absence and (D) presence of thrombin (100 pM). Peaks at m/z 196.967, 393.933, and 590.900 represent $[Au_1]^+$, $[Au_2]^+$, and $[Au_3]^+$ ions, respectively. In total, 1000 pulsed laser shots were applied to accumulate the signals from five LDI target positions under a laser power density of 3.8×10^4 Wcm^{-2}. TBA_{29}−AuNPs were prepared in a biological solution containing 100 μM BSA. Peak intensities are plotted in arbitrary units (a. u.).

and the NCM as the target. Under laser irradiation, the photoabsorption of the AuNPs induced the desorption and ionization of surface atoms. We monitored the presence of cationic clusters ($[Au_x]^+$; x = 1−3) in the mass spectra to determine the degrees of fragmentation and vaporization of the surface atoms of the AuNPs. We attribute the complicated mass spectrum in Figure 1A to the fragmentation of the surface molecules during the desorption and ionization processes under laser irradiation. As a result, the signals of the Au clusters were inhibited through interference from the fragments' signals. The signal-to-noise (S/N) ratio of the signals of the Au clusters in Figure 1A was less than 5. In contrast, the intensities of the many interference peaks were significantly lower in the mass spectrum recorded using TBA_{29}−AuNP/NCM as the matrix (Figure 1C), presumably because nitrocellulose effectively bound the cationic molecules at its negatively charged sites to limit or eliminate their interference during the LDI process.[42,55,56] Only AuNP-derived ions, including $[Au_1]^+$, $[Au_2]^+$, and $[Au_3]^+$, were dominant in this mass spectrum; in contrast, the blank NCM provided a flat mass spectrum (Figure 1B). The S/N ratio of the Au clusters in Figure 1C was greater than 500. The relative standard deviations (RSDs) for the signal fluctuations of these Au cluster ions from TBA_{29}−AuNP/NCM substrates, collected from 50 different mass spectra, were all less than 5%, revealing the samples' high homogeneity. After the addition of thrombin (100 pM), the intensities of the signals for $[Au_1]^+$, $[Au_2]^+$, and $[Au_3]^+$ species decreased to 50, 60, and 90%, respectively (Figure 1D), of their corresponding signals in Figure 1C. The thrombin molecules appeared to stabilize the AuNP surfaces, decreasing the efficiency of desorption and ionization of Au atoms from the AuNP surfaces under pulsed laser irradiation, when bound to the aptamer-conjugated AuNP surfaces through highly selective and strong TBA_{29}−thrombin interactions. Alternatively, competitive ionization of the proteins and the Au clusters, or reactions of the Au clusters with the proteins ions in the gas phase, might also have resulted in the decreases in intensities of the Au cluster signals. From DLS measurements, we estimated the hydrodynamic diameters and zeta potentials of the TBA_{29}−AuNPs (100 pM) in the absence and presence of thrombin (1.0 nM) to be 44.3 (±2.1) nm/−15.2 (±1.1) mV (n = 3) and 55.4 (±4.7) nm/−11.8 (±1.0) mV (n = 3), respectively. The greater hydrodynamic size and lower zeta potential of the latter confirmed that thrombin molecules had bound to the particles' surfaces.

To further support our reasoning, we conducted control experiments using BSA-capped AuNPs (BSA−AuNPs) or random DNA-modified Au NPs (rDNA−AuNPs) under similar conditions. As expected, the addition of thrombin (100 pM) did not induce any significant changes in the signals of the $[Au_x]^+$ cluster ions (see Figure S1 in the Supporting Information). Scanning electron microscopy (SEM) images revealed (see Figure S2 in the Supporting Information) that the TBA_{29}−AuNPs were deposited homogenously on the NCM, with almost identical densities of deposited TBA_{29}−AuNPs on the NCM membranes in the absence and presence of thrombin (1.0 nM), presumably because of the presence of a high concentration of BSA in these solutions. In addition, the average particle size (ca. 13 nm) of the TBA_{29}−AuNPs on the NCM was very similar to that of the original citrate-capped AuNPs. These findings reveal that the variations in the signals of the $[Au_x]^+$ clusters did not result from changes in the homogeneity, deposition density, or particle sizes of the AuNPs during the LDI process. Notably, the signal intensities of the Au cluster ions plateaued after incubation for 2 h. It is possible that more particles diffused into the interior porous network of the NCM during the incubation period, making those AuNPs less susceptible to laser irradiation. Nevertheless, the porous structure of the NCM provided a highly homogeneous deposition of TBA_{29}−AuNPs.

The SPR absorption bands of the TBA_{29}−AuNPs (10 pM) at 520 nm in the absence and presence of 100 pM thrombin (see Figure S3 in the Supporting Information) revealed a slight increase (<3%) in the signal of the latter, due to the change in refractive index of the surroundings of the particle. We also conducted MALDI-MS to detect the thrombin (1.0 nM) using organic matrix, 2,5-dihydroxybenzoic acid (DHB), α-cyano-4-hydroxycinnamic acid (CHCA), or sinapinic acid (SA) for thrombin/TBA_{29}−AuNPs complexes. However, the low efficiency of desorption/ionization of thrombin and/or low concentration of thrombin cause a failure in the performance of MALDI-MS for detecting thrombin (data not shown). Taken

together, our results indicate that using TBA_{29}–AuNP/NCM as a readout platform allowed a selective protein–ligand interaction to be transduced to a highly amplified mass signal, when monitoring the signal from the more-abundant $[Au]^+$ ions rather than that of the less-abundant target protein, yielding a sensitivity much higher than those of optical approaches (e.g., UV–Vis absorption, fluorescence). Notably, the combination of TBA_{29}–AuNP/NCM and SALDI-MS monitoring of the $[Au_1]^+$ signal allowed detection of the TBA_{29}–AuNPs at concentrations as low as 0.05 pM; in contrast, the equivalent concentration was approximately 2.0 pM from UV–Vis absorption measurements (see Figure S4 in the Supporting Information). This SALDI-MS approach allowed the detection of TBA_{29}–AuNPs as low as 0.05 pM because of the large number of surface atoms and high concentration of TBA_{29}–AuNPs on the NCM from a highly dilute aqueous solution. Higher sensitivity would be achieved if lower concentrations of NPs were present.

Parameters for MS Signals. We studied the effect of the laser power density on the analysis of thrombin in LDI-MS. Figure S5A (Supporting Information) reveals that the optimal power density was 3.8×10^4 Wcm^{-2}. Although lower mass spectral backgrounds were generated at lower power density ($<3.8 \times 10^4$ Wcm^{-2}), insufficient energy was absorbed and the ionization efficiency was quite low. To avoid using an excessively high laser power density, which led to higher levels of background noise and loss of resolution, we chose a value of 3.8×10^4 Wcm^{-2} for our experiments. Figure S5B (Supporting Information) indicates that the sensitivity and linearity of the 13-nm AuNPs (10 pM) toward thrombin were greater than those of the 32 or 56 nm AuNPs (10 pM each), presumably because the smaller surface area and higher curvature of the 13 nm TBA_{29}–AuNPs result in greater thrombin enrichment on these AuNPs. In addition, the abundances of higher-order Au clusters increased upon increasing the AuNP diameter (e.g., a signal for $[Au_5]^+$ appeared in the spectrum of the 56 nm TBA_{29}–AuNPs), with the signals of the cluster ions becoming less sensitive to the surface properties. Thus, the 13 nm AuNPs provided higher sensitivity because their surfaces were affected to greater degrees by changes in their surrounding media.

Selectivity and Sensitivity. Next, we evaluated TBA_{29}–AuNP/NCM as an LDI-MS substrate for the analysis of various proteins (thrombin, lysozyme, insulin, conalbumin, myoglobin, catalase, transferrin, carbonic anhydrase; 100 pM for thrombin, 10 nM for each of the other proteins) in the presence of BSA (100 μM). Figure 2 plots the recorded relative signal intensities of the $[Au_1]^+$ ions $[(I_{Au+}{}^0 - I_{Au+})/I_{Au+}{}^0]$ in the absence ($I_{Au+}{}^0$) and presence (I_{Au+}) of proteins; it reveals that this system was highly selective (1000-fold or more) toward thrombin over the other proteins. In addition, the tolerance concentrations of the other proteins were within a relative error range of ±5% during the sensing of thrombin (100 pM) on the TBA_{29}–AuNP/NCM substrate when their concentrations were at least 1000 times greater than the thrombin concentration. The signal intensities of Au cluster ions decreased upon increasing the thrombin concentration to 10 nM (Figure 3A). The detection dynamic range for thrombin extended from 50 fM to 50 nM. The logarithmic plot of the relative signal intensity of the $[Au_1]^+$ ions $[(I_{Au+}{}^0 - I_{Au+})/I_{Au+}{}^0]$ was linear with respect to the thrombin concentration from 100 fM to 10 nM—covering nearly 5 orders of magnitude—with a correlation coefficient greater than 0.98 (Figure 3B). The LOD for thrombin was approximately 50 fM (at a S/N ratio of 3) in the presence of

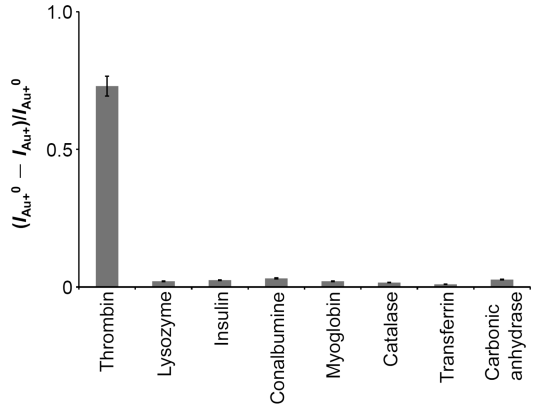

Figure 2. Selectivity of the TBA_{29}–AuNP/NCM substrate in LDI-MS measurements of various proteins in 25 mM Tris-HCl (pH 7.4), 150 mM NaCl, 5.0 mM KCl, 1.0 mM $MgCl_2$, 1.0 mM $CaCl_2$, and 100 μM BSA. Error bars represent standard deviations from five repeated experiments. Other conditions were the same as those described in Figure 1.

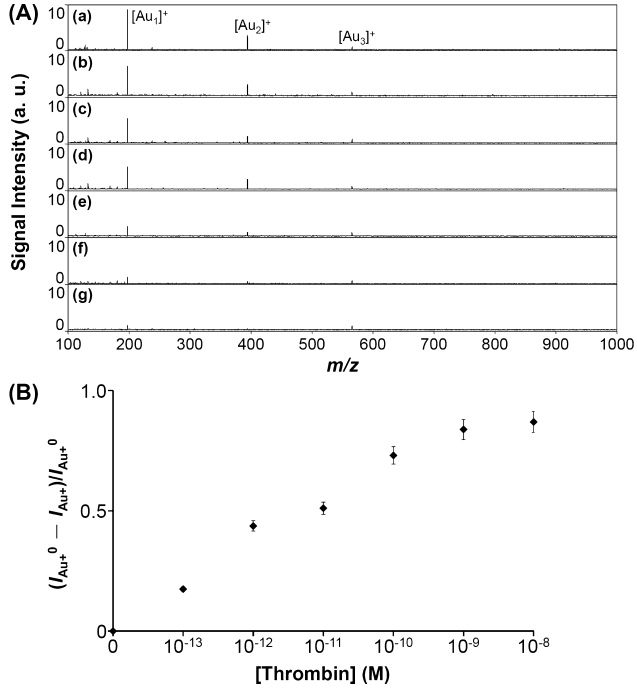

Figure 3. (A) Mass spectra recorded using TBA_{29}–AuNP/NCM (10 pM) as a probe for the detection of (a) 0, (b) 1.0×10^{-13}, (c) 1.0×10^{-12}, (d) 1.0×10^{-11}, (e) 1.0×10^{-10}, (f) 1.0×10^{-9}, and (g) 1.0×10^{-8} M spiked thrombin in a biological buffer containing BSA (100 μM). (B) Relative signal intensity of $[Au_1]^+$ ions $[(I_{Au+}{}^0 - I_{Au+})/I_{Au+}{}^0]$ plotted with respect to the concentration of thrombin (0–10 nM). Other conditions were the same as those described in Figure 1.

100 μM BSA (i.e., a 2×10^9-fold higher concentration). Therefore, we suspected this highly selective sensor to have great potential for detecting thrombin in complex, real samples. This approach provides a sensitivity that is comparable with or higher than those obtained using optical and electrochemical platforms in conjunction with aptamer-modified nanomaterials.[57–67] The ultralow concentration of the probe (TBA_{29}–AuNP), the clean mass spectra, the high affinity of thrombin toward TBA_{29}–AuNPs, and the high level of extraction of thrombin onto the TBA_{29}–AuNP/NCM membrane all

contributed to this system's sensitivity being higher than those obtained for other sensors.

We also tested this Apt−AuNP/NCM−based SALDI-MS approach after conjugation of other aptamers, namely Apt_{PDGF}, AGRO100, and Apt_{Lys}, for the detection of PDGF-BB, nucleolin, and lysozyme, respectively. Figure S6 (Supporting Information) demonstrates that the resulting Apt−AuNP/NCMs allowed the detection of these proteins at concentrations as low as the femtomolar level. Thus, a variety of biological protein−ligand interactions can be transduced to highly amplified signals for Au clusters in LDI mass spectra. Our results suggest that this novel, simple LDI-MS approach using Apt−AuNP/NCM probes might allow identification, with ultrahigh sensitivity, of a wide range of low-abundance analytes in biological samples.

Practicality. To examine the feasibility of our developed approach in practical applications, we used a standard addition method to analyze thrombin (1 pM−10 nM) in 10-fold−diluted human serum samples. Unfortunately, the assay failed to detect thrombin in the serum, mainly because of the matrix effect, due to nonspecific competitive binding of the highly concentrated background proteins in the serum to the NCM. To minimize this interference, we developed an NP-assisted protein enrichment method to concentrate thrombin and remove the matrix. Serum samples (500 μL) diluted by a factor of 10 and thrombin at concentrations ranging from 0 to 10 nM, and TBA_{29}−AuNPs (10 pM) in biological buffer containing BSA (100 μM) were mixed at room temperature for 1 h. The samples were then centrifuged and the supernatants removed; the precipitates were resuspended in biological buffer (pH 7.4, 500 μL) and reacted with the NCM (Figure 4A). The intensity of the signal for the $[Au_1]^+$ ions decreased upon increasing the concentration of spiked thrombin over the range from 1 pM to 10 nM in the 10-fold diluted human serum samples. Using this new approach, we obtained recoveries of 97−104% from these measurements. The LOD for thrombin in this complicated biological sample was approximately 0.2 pM (Figure 4B). Notably, the presence of thiol compounds (e.g., cysteine, homocysteine, glutathione) at micromolar concentrations, proteins (e.g., serum albumin, immunoglobulins) at submillimolar concentrations, and salt (NaCl) at high concentrations (>100 mM) in this complicated sample did not interfere with the probe's performance. Therefore, our TBA_{29}−AuNP/NCM probe is a practical tool for measuring the levels of thrombin in biological samples. The success of our TBA_{29}−AuNP-assisted thrombin enrichment method meant that background proteins did not interfere with the interactions between the TBA_{29}−AuNPs and thrombin. Therefore, the matrix effect observed in the absence of NP-assisted protein enrichment was due to nonspecific competitive binding of the highly concentrated background proteins in the serum to the NCM. Although the sensitivities of some aptamer-based electrochemical sensors have been greater than that of our Apt-AuNP/NCM probe, they have rarely been applied to analyses of thrombin in complicated biological samples.[68−72] In addition, the wide dynamic range of our probe (over 5 orders of magnitude) suggests that it has great potential for use in monitoring the levels of thrombin in the different steps of blood coagulation and in the diagnosis of various diseases associated with coagulation abnormalities.

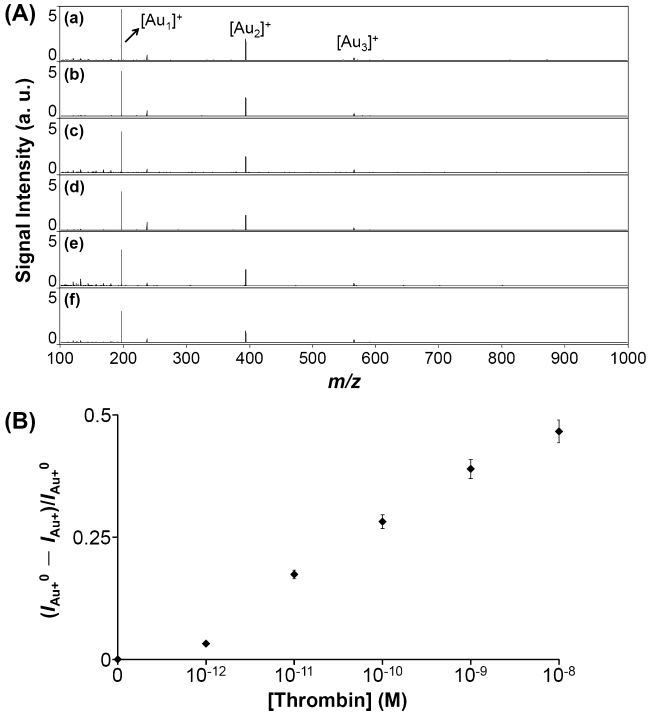

Figure 4. (A) Mass spectra recorded using TBA_{29}−AuNPs/NCM (10 pM) as a probe for the detection of (a) 0, (b) 1.0×10^{-12} M, (c) 1.0×10^{-11} M, (d) 1.0×10^{-10} M, (e) 1.0×10^{-9} M, and (f) 1.0×10^{-8} M thrombin spiked in a 10-fold−diluted serum sample containing a biological buffer and BSA (100 μM). (B) Linearity of the relative signal intensity for $[Au_1]^+$ ions $(I_{Au+}{}^0 - I_{Au+})/I_{Au+}{}^0]$ with respect to the spiked thrombin concentration (0−10 nM). Other conditions were the same as those described in Figure 1.

CONCLUSIONS

TBA_{29}−AuNP/NCM can be used as a novel LDI-MS substrate for the analysis of thrombin in highly complex biological samples (e.g., human serum). After selective capture of the target protein by the surface aptamer units, the particles were isolated through a simple centrifugation process and then deposited onto the NCM to function as a highly efficient background-free SALDI substrate. Under pulsed-laser irradiation, the binding of thrombin inhibited the ability of the TBA_{29}−AuNPs to undergo efficient energy absorption and/or transfer to the surface Au atoms, resulting in low abundances of signals for Au cluster ions in the mass spectra. Accordingly, we used the decrease in the signal intensities of the Au cluster ions as a target-labeling indicator of thrombin. Relative to conventional AuNP-based LDI-MS methodologies, our TBA_{29}−AuNP/NCM probes offer simple sample preparation, higher Au cluster desorption/ionization efficiency, excellent reproducibility, improved repeatability for analytes (RSDs: <5%), lower matrix interference in the mass spectrum, and ultrahigh sensitivity for analytes (down to the femtomolar regime). Because it uses highly selective protein−ligand interactions, this strategy allows a range of biological signals to be amplified merely by decorating other aptamers onto the AuNP surfaces. Moreover, we suspect that the sensitivity of this assay might be improved by optimizing the wavelength or the frequency of the pulsed laser or by using other metallic NPs. Our system also has the potential to enable the use of a series of aptamer-conjugated metallic NPs (e.g., Au, Ag, and Pt NPs) to allow multiple simultaneous detections.

■ ASSOCIATED CONTENT

Supporting Information

Additional information as noted in the text. This material is available free of charge via the Internet at http://pubs.acs.org.

■ AUTHOR INFORMATION

Corresponding Author

*Tel.: 011-886-2-2462-2192, ext. 5517. Fax: 011-886-2-2462-2034. E-mail: huanging@ntou.edu.tw.

Notes

The authors declare no competing financial interest.

■ ACKNOWLEDGMENTS

We thank Yu-Jia Li for her valuable assistance in the negative-mode mass experiments. This study was supported by the National Science Council of Taiwan under contract 99-2113-M-019-001-MY2.

■ REFERENCES

(1) Hashimoto, S.; Werner, D.; Uwada, T. *J. Photochem. Photobiol. C* **2012**, *13*, 28−54.
(2) Myroshnychenko, V.; Rodríguez-Fernández, J.; Pastoriza-Santos, I.; Funston, A. M.; Novo, C.; Mulvaney, P.; Liz-Marzán, L. M.; García de Abajo, F. J. *Chem. Soc. Rev.* **2008**, *37*, 1792−1805.
(3) Dykman, L.; Khlebtsov, N. *Chem. Soc. Rev.* **2012**, *41*, 2256−2282.
(4) Arvizo, R.; Bhattacharya, R.; Mukherjee, P. *Expert Opin. Drug Deliv.* **2010**, *7*, 753−763.
(5) Yeh, Y.-C.; Creran, B.; Rotello, V. M. *Nanoscale* **2012**, *4*, 1871−1880.
(6) Dreaden, E. C.; Alkilany, A. M.; Huang, X.; Murphy, C. J.; El-Sayed, M. A. *Chem. Soc. Rev.* **2012**, *41*, 2740−2779.
(7) Guo, Z.; Ganawi, A. A. A.; Liu, Q.; He, L. *Anal. Bioanal. Chem.* **2006**, *384*, 584−592.
(8) Pilolli, R.; Palmisano, F.; Cioffi, N. *Anal. Bioanal. Chem.* **2012**, *402*, 601−623.
(9) Urban, P. L.; Amantonico, A.; Zenobi, R. *Mass Spectrom. Rev.* **2011**, *30*, 435−478.
(10) Arakawa, R.; Kawasaki, H. *Anal. Sci.* **2010**, *26*, 1229−1240.
(11) Castellana, E. T.; Sherrod, S. D.; Russell, D. H. *J. Assoc. Lab. Autom.* **2008**, *13*, 330−334.
(12) Law, K. P.; Larkin, J. R. *Anal. Bioanal. Chem.* **2011**, *399*, 2597−2622.
(13) Chiang, C.-K.; Chen, W.-T.; Chang, H.-T. *Chem. Soc. Rev.* **2011**, *40*, 1269−1281.
(14) Aminlashgari, N.; Shariatgorji, M.; Ilag, L. L.; Hakkarainen, M. *Anal. Methods* **2011**, *3*, 192−197.
(15) Qiao, L.; Liu, B.; Girault, H. H. *Nanomedicine* **2010**, *5*, 1641−1652.
(16) Watanabe, T.; Kawasaki, H.; Yonezawa, T.; Arakawa, R. *J. Mass Spectrom.* **2008**, *43*, 1063−1071.
(17) Amini, N.; Shariatgorji, M.; Thorsén, G. *J. Am. Soc. Mass Spectrom.* **2009**, *20*, 1207−1213.
(18) Nayak, R.; Knapp, D. R. *Anal. Chem.* **2010**, *82*, 7772−7778.
(19) Bi, H.; Qiao, L.; Busnel, J.-M.; Devaud, V.; Liu, B.; Girault, H. H. *Anal. Chem.* **2009**, *81*, 1177−1183.
(20) Kawasaki, H.; Yao, T.; Suganuma, T.; Okumura, K.; Iwaki, Y.; Yonezawa, T.; Kikuchi, T.; Arakawa, R. *Chem.—Eur. J.* **2010**, *16*, 10832−10843.
(21) Kawasaki, H.; Akira, T.; Watanabe, T.; Nozaki, K.; Yonezawa, T.; Arakawa, R. *Anal. Bioanal. Chem.* **2009**, *395*, 1423−1431.
(22) Gholipour, Y.; Giudicessi, S. L.; Nonami, H.; Erra-Balsells, R. *Anal. Chem.* **2010**, *82*, 5518−5526.
(23) Wang, M.-T.; Liu, M.-H.; Wang, C. R. C.; Chang, S. Y. *J. Am. Soc. Mass Spectrom.* **2009**, *20*, 1925−1932.
(24) Kuo, T.-R.; Chen, J.-S.; Chiu, Y.-C.; Tsai, C.-Y.; Hu, C.-C.; Chen, C.-C. *Anal. Chim. Acta* **2011**, *699*, 81−86.
(25) Wu, H.-P.; Yu, C.-J.; Lin, C.-Y.; Lin, Y.-H.; Tseng, W.-L. *J. Am. Soc. Mass Spectrom.* **2009**, *20*, 875−882.
(26) McLean, J. A.; Stumpo, K. A.; Russell, D. H. *J. Am. Chem. Soc.* **2005**, *127*, 5304−5305.
(27) Castellana, E. T.; Gamez, R. C.; Gómez, M. E.; Russell, D. H. *Langmuir* **2010**, *26*, 6066−6070.
(28) Inuta, M.; Arakawa, R.; Kawasaki, H. *Analyst* **2011**, *136*, 1167−1176.
(29) Shibamoto, K.; Sakata, K.; Nagoshi, K.; Korenaga, T. *J. Phys. Chem. C* **2009**, *113*, 17774−17779.
(30) Spencer, M. T.; Furutani, H.; Oldenburg, S. J.; Darlington, T. K.; Prather, K. A. *J. Phys. Chem. C* **2008**, *112*, 4083−4090.
(31) Lin, Y.-W.; Chen, W.-T.; Chang, H.-T. *Rapid Commun. Mass Spectrom.* **2010**, *24*, 933−938.
(32) Yan, B.; Zhu, Z.-J.; Miranda, O. R.; Chompoosor, A.; Rotello, V. M.; Vachet, R. W. *Anal. Bioanal. Chem.* **2010**, *396*, 1025−1035.
(33) Tang, J.; Liu, Y.; Qi, D.; Yao, G.; Deng, C.; Zhang, X. *Proteomics* **2009**, *9*, 5046−5055.
(34) Kawasaki, H.; Sugitani, T.; Watanabe, T.; Yonezawa, T.; Moriwaki, H.; Arakawa, R. *Anal. Chem.* **2008**, *80*, 7524−7533.
(35) Tanaka, K. A.; Key, N. S.; Levy, J. H. *Anesth. Analg.* **2009**, *108*, 1433−1446.
(36) Siller-Matula, J. M.; Schwameis, M.; Blann, A.; Mannhalter, C.; Jilma, B. *Thromb. Haemost.* **2011**, *106*, 1020−1033.
(37) Green, D.; Karpatkin, S. *Cell Cycle* **2010**, *9*, 656−661.
(38) Al Dieri, R.; Peyvandi, F.; Santagostino, E.; Giansily, M.; Mannucci, P. M.; Schved, J. F.; Béguin, S.; Hemker, H. C. *Thromb. Haemost.* **2002**, *88*, 576−582.
(39) Allen, G. A.; Wolberg, A. S.; Oliver, J. A.; Hoffman, M.; Roberts, H. R.; Monroe, D. M. *J. Thromb. Haemost.* **2004**, *2*, 402−413.
(40) Dargaud, Y.; Béguin, S.; Lienhart, A.; Al Dieri, R.; Trzeciak, C.; Bordet, J. C.; Hemker, H. C.; Negrier, C. *Thromb. Haemost.* **2005**, *93*, 475−480.
(41) Tasset, D. M.; Kubik, M. F.; Steiner, W. *J. Mol. Biol.* **1997**, *272*, 688−698.
(42) Liu, Y.-C.; Chiang, C.-K.; Chang, H.-T.; Lee, Y.-F.; Huang, C.-C. *Adv. Funct. Mater.* **2011**, *21*, 4448−4455.
(43) Storhoff, J. J.; Elghanian, R.; Mucic, R. C.; Mirkin, C. A.; Letsinger, R. L. *J. Am. Chem. Soc.* **1998**, *120*, 1959−1964.
(44) Demers, L. M.; Mirkin, C. A.; Mucic, R. C.; Reynolds, R. A.; Letsinger, R. L.; Elghanian, R.; Viswanadham, G. *Anal. Chem.* **2000**, *72*, 5535−5541.
(45) The Handbook, http://www.probes.com/handbook/sections/0803.html. (accessed September 2012).
(46) Shiang, Y.-C.; Huang, C.-C.; Wang, T.-H.; Chien, C.-W.; Chang, H.-T. *Adv. Funct. Mater.* **2010**, *20*, 3175−3182.
(47) Liao, Y.-J.; Shiang, Y.-C.; Huang, C.-C.; Chang, H.-T. *Langmuir* **2012**, *28*, 8944−8951.
(48) Du, Y.; Li, B.; Wang, E. *Bioanal. Rev.* **2010**, *1*, 187−208.
(49) Zhao, Q.; Lu, X.; Yuan, C.-G.; Li, X.-F.; Le, X. C. *Anal. Chem.* **2009**, *81*, 7484−7489.
(50) Hsu, C.-L.; Wei, S.-C.; Jian, J.-W.; Chang, H.-T.; Chen, W.-H.; Huang, C.-C. *RCS. Adv.* **2012**, *2*, 1577−1584.
(51) Gershoni, J. M. *Trends Biochem. Sci.* **1985**, *10*, 103−106.
(52) Vogel, M.; Herlert, A.; Schweikhard, L. *J. Am. Soc. Mass Spectrom.* **2003**, *14*, 614−621.
(53) Moini, M.; Eyler, J. R. *J. Chem. Phys.* **1988**, *88*, 5512 (4 pages).
(54) Vogel, M.; Herlert, A.; Schweikhard, L. *J. Am. Soc. Mass Spectrom.* **2003**, *14*, 614−621.
(55) Picariello, G.; Romano, R.; Addeo, F. *Anal. Chem.* **2010**, *82*, 5783−5791.
(56) Luque-Garcia, J. L.; Zhou, G.; Sun, T.-T.; Neubert, T. A. *Anal. Chem.* **2006**, *78*, 5102−5108.
(57) Wang, W.; Chen, C.; Qian, M.; Zhao, X. S. *Anal. Biochem.* **2008**, *373*, 213−219.
(58) Pavlov, V.; Xiao, Y.; Shlyahovsky, B.; Willner, I. *J. Am. Chem. Soc.* **2004**, *126*, 11768−11769.
(59) Chen, X.; Liu, H.; Zhou, X.; Hu, J. *Nanoscale* **2010**, *2*, 2841−2846.

(60) Wang, Y.; Li, D.; Ren, W.; Liu, Z.; Dong, S.; Wang, E. *Chem. Commun.* **2008**, *22*, 2520−2522.
(61) Xu, H.; Mao, X.; Zeng, Q.; Wang, S.; Kawde, A.; Liu, G. *Anal. Chem.* **2009**, *81*, 669−675.
(62) Xia, F.; Zuo, X.; Yang, R.; Xiao, Y.; Kang, D.; Vallée-Bélisle, A.; Gong, X.; Yuen, J. D.; Hsu, B. B. Y.; Heeger, A. J.; Plaxco, K. W. *Proc. Natl. Acad. Sci. U.S.A.* **2010**, *107*, 10837−10841.
(63) Li, F.; Li, J.; Wang, C.; Zhang, J.; Li, X.-F.; Le, X. C. *Anal. Chem.* **2011**, *83*, 6464−6467.
(64) Zhu, D.; Luo, J.; Rao, X.; Zhang, J.; Cheng, G.; He, P.; Fang, Y. *Anal. Chim. Acta* **2012**, *711*, 91−96.
(65) Zhou, W. J.; Halpern, A. R.; Seefeld, T. H.; Corn, R. M. *Anal. Chem.* **2012**, *84*, 440−445.
(66) Kwon, M. J.; Lee, J.; Wark, A. W.; Lee, H. J. *Anal. Chem.* **2012**, *84*, 1702−1707.
(67) Guo, L.; Ferhan, A. R.; Lee, K.; Kim, D.-H. *Anal. Chem.* **2011**, *83*, 2605−2612.
(68) Wang, Y.; Bao, L.; Liu, Z.; Pang, D. W. *Anal. Chem.* **2011**, *83*, 8130−8137.
(69) Zhang, J.; Chen, P.; Wu, X.; Chen, J.; Xu, L.; Chen, G.; Fu, F. *Biosens. Bioelectron.* **2011**, *26*, 2645−2650.
(70) Li, Y.; Qi, H.; Gao, Q.; Yang, J.; Zhang, C. *Biosens. Bioelectron.* **2010**, *26*, 754−759.
(71) Zhao, J.; Zhang, Y.; Li, H.; Wen, Y.; Fan, X.; Lin, F.; Tan, L.; Yao, S. *Biosens. Bioelectron.* **2011**, *26*, 2297−2303.
(72) Chai, Y.; Tian, D.; Cui, H. *Anal. Chim. Acta* **2012**, *715*, 86−92.